ISSN 1674-1056
http://cpb.iphy.ac.cn
http://iopscience.iop.org/cpb
中国物理 B
Chinese Physics
中国物理 Chinese Physics B

Microstructure and magnetocaloric properties in melt-spun and high-pressure hydrogenated $La_{0.5}Pr_{0.5}Fe_{11.4}Si_{1.6}$ ribbons

Qian Liu(刘倩), Min Tong(佟敏), Xin-Guo Zhao(赵新国), Nai-Kun Sun(孙乃坤), Xiao-Fei Xiao(肖小飞), Jie Guo(郭杰), Wei Liu(刘伟), and Zhi-Dong Zhang(张志东)

Citation: Chin. Phys. B, 2021, 30 (**8**): 087502. DOI: 10.1088/1674-1056/abea91
Journal homepage: http://cpb.iphy.ac.cn; http://iopscience.iop.org/cpb

What follows is a list of articles you may be interested in

Magnetic properties and resistivity of a 2:17-type SmCo magnet doped with ZrO_2

Qi-Qi Yang(杨棋棋), Zhuang Liu(刘壮), Chao-Yue Zhang(张超越), Hai-Chen Wu(吴海辰), Xiao-Lei Gao(高晓磊), Yi-Long Ma(马毅龙), Ren-Jie Chen(陈仁杰), and A-Ru Yan(闫阿儒)

Chin. Phys. B, 2021, 30 (**7**): 077504. DOI: 10.1088/1674-1056/abf7a9

Effects of post-sinter annealing on microstructure and magnetic properties of Nd-Fe-B sintered magnets with Nd-Ga intergranular addition

Jin-Hao Zhu(朱金豪), Lei Jin(金磊), Zhe-Huan Jin(金哲欢), Guang-Fei Ding(丁广飞), Bo Zheng(郑波), Shuai Guo(郭帅), Ren-Jie Chen(陈仁杰), and A-Ru Yan(闫阿儒)

Chin. Phys. B, 2021, 30 (**6**): 067503. DOI: 10.1088/1674-1056/abddad

Effect of hydrogen plasma implantation on the micro-structure and magnetic properties of hcp-$Co_{80}{}^{57}Fe_4Ir_{16}$ thin films

Hui Wang(王辉), Meng Wu(吴猛), Haiping Zhou(周海平), Bo Zhang(张博), Shixin Hu(胡世欣), Tianyong Ma(马天勇), Zhiwei Li(李志伟), Liang Qiao(乔亮), Tao Wang(王涛), and Fashen Li(李发伸)

Chin. Phys. B, 2021, 30 (**5**): 057505. DOI: 10.1088/1674-1056/abe0c3

Enhanced spin-orbit torque efficiency in $Pt_{100-x}Ni_x$ alloy based magnetic bilayer

Congli He(何聪丽), Qingqiang Chen(陈庆强), Shipeng Shen(申世鹏), Jinwu Wei(魏晋武), Hongjun Xu(许洪军), Yunchi Zhao(赵云驰), Guoqiang Yu(于国强), and Shouguo Wang(王守国)

Chin. Phys. B, 2021, 30 (**3**): 037503. DOI: 10.1088/1674-1056/abe3f4

Nanocrystalline and nanocomposite permanent magnets by melt spinning technique

Chuanbing Rong(荣传兵), Baogen Shen(沈保根)

Chin. Phys. B, 2018, 27 (**11**): 117502. DOI: 10.1088/1674-1056/27/11/117502

Microstructure and magnetocaloric properties in melt-spun and high-pressure hydrogenated $La_{0.5}Pr_{0.5}Fe_{11.4}Si_{1.6}$ ribbons*

Qian Liu(刘倩)[1,2], Min Tong(佟敏)[1], Xin-Guo Zhao(赵新国)[1,2,†], Nai-Kun Sun(孙乃坤)[3,‡], Xiao-Fei Xiao(肖小飞)[1,2], Jie Guo(郭杰)[1,2], Wei Liu(刘伟)[1,2], and Zhi-Dong Zhang(张志东)[1,2]

[1] *Shenyang National Laboratory for Materials Science, Institute of Metal Research, Chinese Academy of Sciences, Shenyang* 110016, *China*
[2] *School of Materials Science and Engineering, University of Science and Technology of China, Shenyang* 110016, *China*
[3] *School of Science, Shenyang Ligong University, Shenyang* 110159, *China*

(Received 24 December 2020; revised manuscript received 25 January 2021; accepted manuscript online 1 March 2021)

The effects of wheel speeds and high-pressure hydrogen treatment on phase evolution, microstructure, and magnetocaloric properties in $La_{0.5}Pr_{0.5}Fe_{11.4}Si_{1.6}$ melt-spun ribbons are studied in this work. The results reveal that the increase of wheel speed is beneficial to the formation of cubic $NaZn_{13}$-type phase and the grain refinement. The optimized wheel speed for microstructural and magnetocaloric properties is 30 m/s. The largest entropy change of 18.1 J/kg·K at 190 K under a magnetic field change of 0 T–5 T is obtained in $La_{0.5}Pr_{0.5}Fe_{11.4}Si_{1.6}$ ribbons melt-spun at 30 m/s. After a high-pressure hydrogen treatment of 50 MPa, the Curie temperature of the ribbons prepared at 30 m/s is adjusted to about 314 K and the large $-\Delta S_M$ of 17.9 J/kg·K under a magnetic field change of 0 T–5 T is achieved at room temperature with almost none hysteresis loss. The small thermal and magnetic hysteresis and the large $-\Delta S_M$ make the $La_{0.5}Pr_{0.5}Fe_{11.4}Si_{1.6}$ hydride ribbons appropriate for magnetic refrigerant applications around room temperature.

Keywords: La–Pr–Fe–Si, melt-spun ribbon, hydrides, magnetic properties, microstructure

PACS: 75.30.Sg **DOI:** 10.1088/1674-1056/abea91

1. Introduction

The refrigeration technology plays an important role in contemporary society, which can be used in various fields in daily life and high technologies. The magnetic refrigeration serving at/around room temperature, based on the magnetocaloric effect (MCE), is considered to be a promising alternative to gas compression refrigeration.[1–3] Various magnetic materials, such as $Gd_5(Si_xGe_{1-x})_4$,[1] $MnFeP_{1-x}As_x$,[2] and the hydride of $La(Fe_xSi_{1-x})_{13}$[3–5] possess large magnetic entropy changes around room temperature, accompanying with a first-order magnetic transition (FOMT). Among them, the hydrides of $La(Fe_xSi_{1-x})_{13}$ compounds have attracted particular interest most, because of non-toxic components, environmental friendliness, and tunable Curie temperature.[6,7]

However, it is necessary to add Si or Al to stabilize a $NaZn_{13}$-type La–Fe phase, and it is hard to prepare $LaFe_{13}$ binary compound, since the enthalpy formed between La and Fe is positive. For instance, a stable $NaZn_{13}$-type structure can be formed by substituting a small amount of Si ($1.0 < x < 1.6$) for Fe. The lower the Si content, the more difficultly the stable single-phase alloy of $NaZn_{13}$-type structure can form.[8] The $La(Fe_xSi_{1-x})_{13}$ alloys prepared by conventional casting methods are composed of α-Fe and La–Fe–Si phases, which are caused by the melting upon cooling. According to the La–Fe–Si equilibrium phase diagram,[8] α-Fe dendrites precipitate as primary phase firstly, and then a peritectic reaction with the surrounding liquid occurs to form 1:13 phase (α-Fe + $L_{La} \rightarrow$ 1:13 phase). Therefore, it is essential to implement a high-temperature annealing treatment for the cast $LaFe_{13-x}Si_x$ alloy after having melted in an arc furnace to form the La–Fe–Si phase with the $NaZn_{13}$-type structure, which can accelerate the peritectoid reaction between α-Fe phase and LaFeSi phase. It is usually requisite to perform a lengthy annealing treatment (about 30 days) to ensure homogenization of alloys.[9–11] In order to overcome such a difficulty, it is proposed that the directional solidification technology can directly obtain a large number of 1:13 phases.[12] The rapid solidification inhibits the formation of incipient iron phase and speeds up atomic diffusion during heat treatment. Indeed, it is an important method for the preparation of magnetic materials, which can refine the microstructure, enlarge the solid solubility, reduce the annealing time, and form a metastable phase. Yan *et al.*[13] studied the content change of 1:13 phase in $LaFe_{11.57}Si_{1.43}$ ribbons and found that a large number of 1:13 phase can be obtained by annealing in a short time. Yang *et al.*[14] and Hou *et al.*[15] studied the effects of different cooling rates and annealing times on the phase structure and magnetocaloric properties in La–Ce–Fe–Si alloys. The optimal cooling rate and annealing time are 25 m/s and 20 min at 1273 K, respectively.

On the other hand, in materials with large MCEs there

*Project supported by the National Natural Science Foundation of China (Grant No. 51771197), the Fund from the Chinese Academy of Sciences (Grant No. KJZD-EW-M05), and the Liaoning Revitalization Talents Program, China (Grant No. XLYC1807122).

†Corresponding author. E-mail: xgzhao@imr.ac.cn
‡Corresponding author. E-mail: naikunsun@163.com

© 2021 Chinese Physical Society and IOP Publishing Ltd

usually exist serious thermal hysteresis problems due to the nature of the first-order magnetic phase transition. The large hysteresis losses are certainly harmful for practical applications.[16] The element doping or the introduction of interstitial atom is an effective way to reduce or even eliminate the hysteresis loss of $LaFe_{13-x}Si_x$ compounds. It was found that Co doping in $LaFe_{13-x}Si_x$ alloys can effectively increase Curie temperature and obviously reduce hysteresis loss, but result in relatively low magnetic entropy change.[17,18] The introduction of interstitial H atoms has the same effect on Curie temperature and hysteresis loss, while it has little effect on its phase structure and magnetocaloric properties.[19] In previous work, we reported the effect of high-pressure H_2 treatment of 50 MPa on the $La_{0.5}Pr_{0.5}Fe_{11.4}Si_{1.6}$ flake alloy. The results revealed the desorption of H atoms was significantly weakened after having been treated by high pressure hydrogenation.[20]

In this work, $La_{0.5}Pr_{0.5}Fe_{11.4}Si_{1.6}$ ribbons are prepared by the melt-spun method in different wheel speeds and subsequent annealing, hydrogenation sintering at a high pressure of H_2 gas. The microstructure, phase evolution and magnetocaloric properties of the La–Pr–Fe–Si ribbons are investigated in details under different process conditions.

2. Experiment

La–Pr–Fe–Si ingots with a nominal composition of $La_{0.5}Pr_{0.5}Fe_{11.4}Si_{1.6}$ were fabricated by arc melting in an argon gas atmosphere. The purities of the starting materials were 99.9% for La, 99.9% for Pr, 99.99% for Fe, and 99.999% for Si. The ingots were re-melted four times to ensure the obtainment of a homogenized alloy. We prepared the melt-spun ribbons with different speeds of 10, 20, 30, and 40 m/s by using a rotating copper wheel. The size of ribbons is about 5 mm in width and 100 μm in thickness. The as-spun ribbons were sealed in quartz tubes under a high vacuum and annealed at 1273 K for 2 h and then quenched in ice water. Hydrogenation sintering of $La_{0.5}Pr_{0.5}Fe_{11.4}Si_{1.6}$ ribbons was carried out at 723 K for 2 h in a high pressure H_2 atmosphere of 50 MPa.

The phase characteristics of the ribbons were obtained by x-ray diffraction (XRD). The microstructural analysis was performed by using the backscattered electron (BSE) mode in the scanning electron microscope (SEM). The chemical composition of each phase was determined by energy-dispersive spectroscopy (EDS). Magnetic properties were measured by using a superconducting quantum interference device (SQUID, Quantum Design) magnetometer. The Curie temperature, T_C, was determined from the extreme values of the temperature derivative of the magnetization dM/dT. The magnetic entropy change, $\Delta S_M(T,H)$, was calculated from the thermodynamic Maxwell relationship according to the following equation:[6]

$$\Delta S_M(T,H) = \mu_0 \int_0^H \left(\frac{\partial M}{\partial T}\right)_H dH. \quad (1)$$

3. Results and discussion

Figure 1 shows the XRD patterns at room temperature of the as-spun $La_{0.5}Pr_{0.5}Fe_{11.4}Si_{1.6}$ ribbons prepared at different wheel speeds, the annealed and hydrogenated ribbons at 30 m/s. It is found that ribbons melt-spun at 10 m/s consist of cubic $NaZn_{13}$-type (denoted as 1:13 phase) and α-Fe phases with a slight amount of LaFeSi phase (marked as 1:1:1 phase). It indicates that the 1:13 phase can be formed directly from the liquid by being rapidly solidified. For ribbons prepared at 20 m/s, the content of 1:13 phase increases while a large amount of α-Fe still exists with a minor 1:1:1 phase. It is worth noting that the intensity of α-Fe phase greatly decreases with the increase of wheel speed, and drops to a lowest value at 30 m/s and the 1:1:1 phase almost disappears. The annealed and hydrogenated ribbon (as-spun at 30 m/s) consists of the 1:13 main phase and a little α-Fe as impurity phase. It is noticed that the diffraction peaks of the 1:13 phase shift toward lower angles, indicating lattice expansion in the ribbons after having been hydrogenated. As the wheel speed further increases, the intensity of the α-Fe peak for the alloy melt-spun at 40 m/s is slightly higher than that at 30 m/s. The content of the 1:13 phase related to the wheel speed can be explained by solidification process for the $La_{0.5}Pr_{0.5}Fe_{11.4}Si_{1.6}$ alloy. There exists a mechanism of competing nucleation between Fe phase and 1:13 phases during rapid solidification. The temperature at 707 K is a critical undercooling degree of $LaFe_{11.6}Si_{1.4}$ alloy during rapid solidification, which determines that the phase nucleates preferentially. When the undercooling degree is above 707 K for $LaFe_{11.6}Si_{1.4}$, the 1:13 phase is formed preferentially because of its higher nucleation rate than α-Fe's.[21]

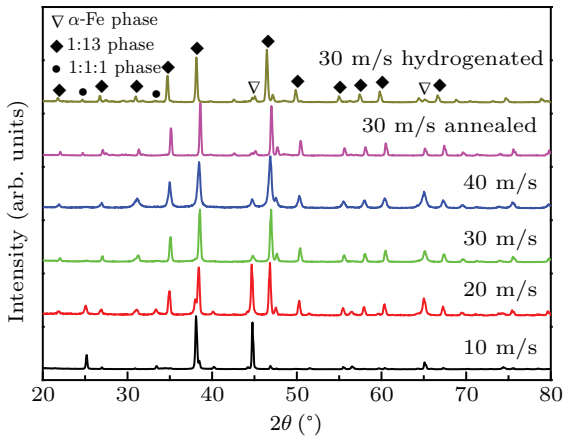


Fig. 1. XRD patterns of $La_{0.5}Pr_{0.5}Fe_{11.4}Si_{1.6}$ melt-spun ribbons prepared at 10 m/s, 20 m/s, 30 m/s, 40 m/s, and the annealed and hydrogenated ribbons melt-spun at 30 m/s.

A larger undercooling is obtained by a faster wheel speed. Similarly, the content of 1:13 phase will increase with the wheel speed increasing. However, continuous increase of the wheel speed is unfavorable for the atomic diffusion and hinders the 1:13 phase from forming due to the introduction of defects.

Figure 2 represents the SEM backscattered electron images of the $La_{0.5}Pr_{0.5}Fe_{11.4}Si_{1.6}$ ribbons melt-spun at (a) 10 m/s, (b) 20 m/s, (c) 30 m/s, and (d) 40 m/s, respectively. The ribbon prepared at 10 m/s contains a large number of dendrites of α-Fe, with black area containing the composition of $La_{1.01}Pr_{0.91}Fe_{94.35}Si_{3.73}$ (at.%), and some La-rich 1:1:1 phases, with white area containing the composition of $La_{17.93}Pr_{15.13}Fe_{37.45}Si_{29.49}$ (at.%) at grain boundary, which are analyzed by the EDS. The formation of a large amount of α-Fe is due to its lower cooling rate, which makes Fe be in a primary phase.[24] At the same time, a certain number of 1:13 phases, with gray area containing the composition of $La_{3.89}Pr_{3.64}Fe_{81.37}Si_{11.10}$ (at.%), is formed through the peritectic reaction under this condition. When the wheel speed increases to 20 m/s, the dendrites of α-Fe and La-rich 1:1:1 phase degenerate into ones with small size obviously and the content of 1:13 phase increases. For the ribbons prepared with faster wheel speeds (30 m/s and 40 m/s), there appears the almost pure 1:13 phase with gray color, while the α-Fe and La-rich 1:1:1 phases are hardly observed in the backscattered electron images. This is due to the fact that the large enough undercooling degree helps to drive the nucleation to form the 1:13 phase. At this undercooling degree, the 1:13 single phase directly forms from the $La_{0.5}Pr_{0.5}Fe_{11.4}Si_{1.6}$ liquid and crosses the two-phase region of α-Fe phase and La-rich liquid phase in the melt spinning process.[22] As seen in Figs. 2(c) and 2(d), with the increase of cooling rate, the crystal grains of 1:13 phase are refined continuously, and the grains are too small to be distinguished clearly by the backscatter image of the SEM for the sample obtained at 40 m/s. This means that the increase of cooling rate is beneficial to the formation of 1:13 phase and the refinement of grain size. Based on the results of XRD and microstructural analysis, the 30 m/s is considered to be the optimized wheel speed in $La_{0.5}Pr_{0.5}Fe_{11.4}Si_{1.6}$ ribbons, which is expected to have a good magnetocaloric properties. The results above mentioned are basically in consistent with those reported by Yang *et al.*[14]

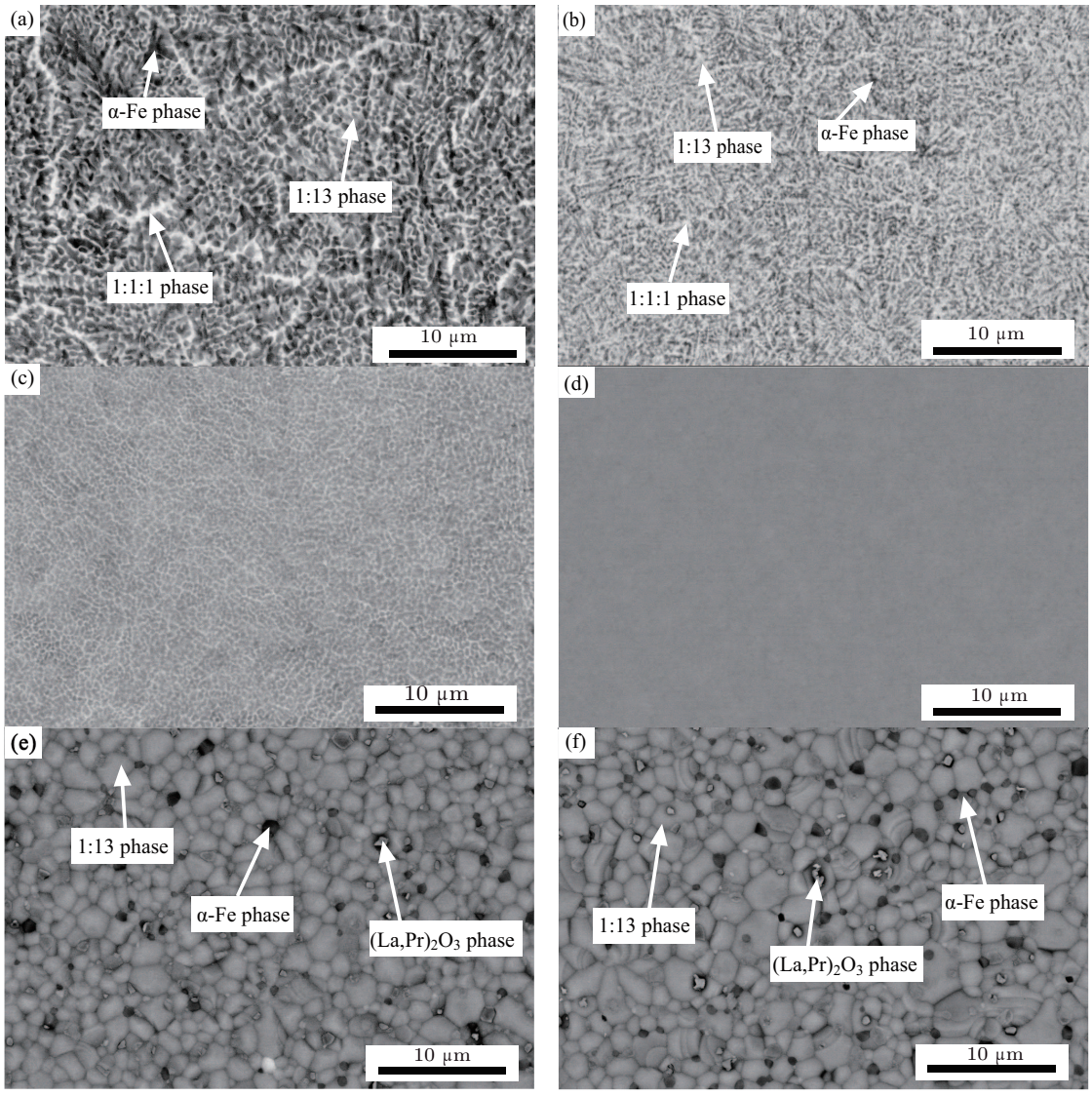


Fig. 2. SEM backscattered electron images of $La_{0.5}Pr_{0.5}Fe_{11.4}Si_{1.6}$ melt-spun ribbons prepared at different wheel speeds: (a) 10 m/s, (b) 20 m/s, (c) 30 m/s, (d) 40 m/s, and (e) annealed and (f) hydrogenated ribbons at wheel speed 30 m/s.

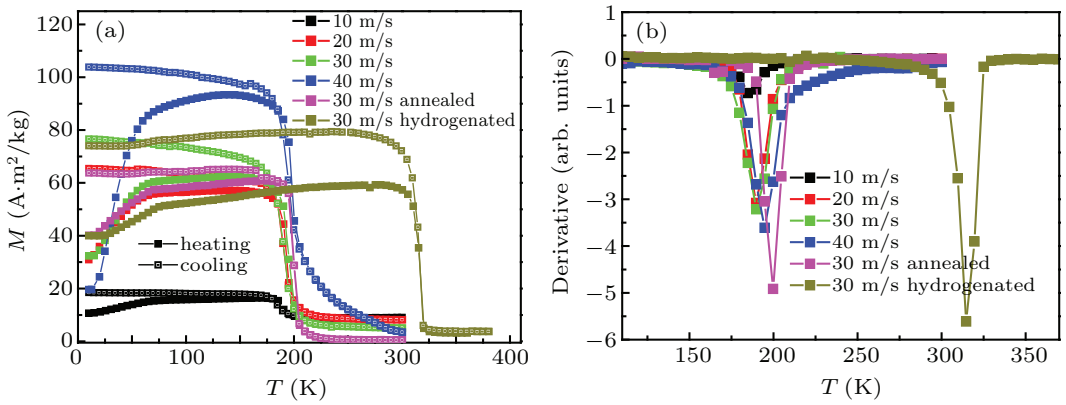


Fig. 3. (a) Magnetization curves as a function of temperature in zero field cooling (ZFC) process and field cooling (FC) process in $La_{0.5}Pr_{0.5}Fe_{11.4}Si_{1.6}$ melt-spun ribbons at wheel speed of 10 m/s, 20 m/s, 30 m/s, 40 m/s; the annealed and hydrogenated ribbons for wheel speed 30 m/s, and (b) corresponding $dM/dT(T)$ curves in FC processes for all the samples.

Figures 2(e) and 2(f) illustrate the SEM backscattered electron images of the $La_{0.5}Pr_{0.5}Fe_{11.4}Si_{1.6}$ ribbons annealed and hydrogenated after being melt-spun at 30 m/s, respectively. It is obvious that the grains grow up after being annealed and α-Fe precipitated in grain boundary with a smaller size. The small white particles on the surface are oxides of rare-earth La–Pr as analyzed by EDS. The element of La–Pr is separated from the grain boundary and oxidized during heat treatment and finally falls out of the surface. It is clear that the presence of oxides on the surface is unbeneficial to the actual magnetic refrigeration.[15] The hydrogenated ribbons have a similar backscatter image, while their grains are slightly larger than those annealed ribbons' due to the growth of grains during hydrogenation treatment.

Figure 3 displays the magnetization curves as a function of temperature in $La_{0.5}Pr_{0.5}Fe_{11.4}Si_{1.6}$ melt-spun ribbons, measured in a magnetic field of 0.01 T in zero field cooling (ZFC) process and field cooling (FC) process. The ribbon samples each have a sharp change in magnetization around T_C indicating a first-order ferromagnetic (FM)/paramagnetic (PM) phase transition. After this transition, the magnetization of the as-spun ribbons does not decrease to zero above T_C. It is an evidence of the existence of α-Fe phase. For the as-spun ribbons prepared with different wheel speeds, the magnetization after the transition decreases with the wheel speed increasing and reaches a minimum value at 30 m/s which corresponds to the least content of the α-Fe phase. The Curie temperature T_C determined from the curves for the minimum of the dM/dT *versus* T in the FC process, is about 184 K, 190 K, 190 K, 194 K for the as-spun ribbons prepared at a wheel speed of 10 m/s, 20 m/s, 30 m/s, and 40 m/s, respectively, as shown in Fig. 3(b). The T_C increases slightly with the increase of wheel speed, which is ascribed to more Si dissolved in the 1:13 phase when the cooling rate increases.[13] As indicated by analyzing the EDS, the compositions of the samples prepared at 20 m/s, 30 m/s, and 40 m/s are $La_{3.99}Pr_{3.58}Fe_{81.10}Si_{11.33}$, $La_{3.92}Pr_{3.51}Fe_{80.97}Si_{11.60}$, and $La_{3.79}Pr_{3.53}Fe_{80.96}Si_{11.72}$ (at.%), respectively. However, it is worth noting that the $M(T)$ curve of the ribbon melt-spun at 40 m/s is slightly different from those of other samples, each of which has a broader transition in the $M(T)$ curve. The phenomenon may be attributed to the increase of defects in the sample.

For the ribbons prepared at a wheel speed of 30 m/s and then treated by annealing and hydrogenation, their magnetization is close to zero after completing the magnetic transition. The Curie temperature T_C is found to be 190 K, 199 K, and 314 K for the ribbons melt-spun at 30 m/s, melt-spun at 30 m/s and then annealed, and finally hydrogenated, as shown in Fig. 3(b). The Curie temperature slightly increases after annealing treatment because of the relatively low Fe content in the 1:13 phase. It was proposed by Fujieda *et al.*[23] that the $NaZn_{13}$-type phase formed first with a relatively high Fe content and then its Fe content decreased due to the composition homogenization after having been treated by annealing. After a high pressure hydrogenation treatment, the Curie temperature of the ribbon samples, which is slightly higher than room temperature, increases significantly. The increasing of T_C is related to the quantity of hydrogen atoms in the ribbons. This is because the interstitial H atoms make the lattice expand, which narrows the Fe 3d band and reduces the overlap of Fe 3d wave functions.[24]

Figure 4 shows the variations of the magnetic entropy with temperatures under a field change of 0 T–5 T for $La_{0.5}Pr_{0.5}Fe_{11.4}Si_{1.6}$ ribbons melt-spun different wheel speeds. The peak values of $-\Delta S_M$ are calculated to be about 8.2 J/kg·K, 11.3 J/kg·K, 18.1 J/kg·K, 14.2 J/kg·K for the ribbons prepared at 10 m/s, 20 m/s, 30 m/s, 40 m/s, respectively. With the increase of wheel speed, the value of $-\Delta S_M$ increases significantly. The $-\Delta S_M$ value of the ribbon for 30 m/s is the highest, while it decreases at a higher wheel speed of 40 m/s. This change is ascribed to the quantity of 1:13 phases in the ribbons. The maximum values of $-\Delta S_M$ for a field change of 0 T–5 T are 17.3 J/kg·K and 17.9 J/kg·K, respectively, for the annealed and hydrogenated ribbons after being as-spun at 30 m/s. It is worthwhile to note that the entropy change

of annealed and hydrogenated ribbons all retain a relatively large $-\Delta S_M$ around T_C. It is obvious that the large $-\Delta S_M$ in $La_{0.5}Pr_{0.5}Fe_{11.4}Si_{1.6}$ ribbon is attributed to a field-induced itinerant-electron metamagnetic (IEM) transition from the PM to the FM state above T_C.[25] The results are consistent with previous experimental studies which showed that MCE still maintained at a high value after having been hydrogenated.[18] In a high pressure (50 MPa) hydrogenation treatment, the hydrogen absorption is achieved which leads the H atoms to occupy the interstitial 48f and/or 24d sites in La $(Fe_xSi_{1-x})_{13}$ unit cell.[26,27] The samples of 30 m/s have good magnetocaloric properties before and after heat treatment. So in the following, we will carry out a detailed analysis on the magnetic properties of samples prepared at 30 m/s.

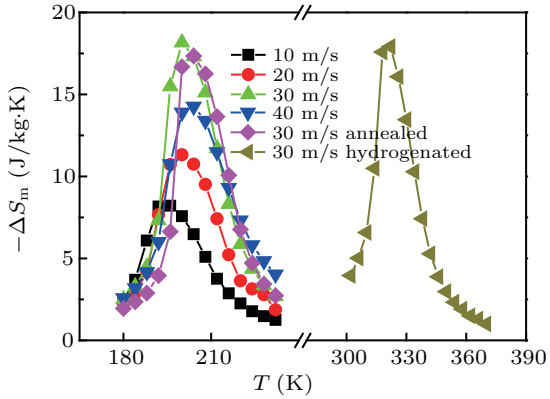


Fig. 4. Temperature-dependent magnetic entropy change under a magnetic field change of 0 T–5 T for $La_{0.5}Pr_{0.5}Fe_{11.4}Si_{1.6}$ melt-spun ribbons prepared at different wheel speeds, and annealed and hydrogenated ribbons prepared at wheel speed 30 m/s.

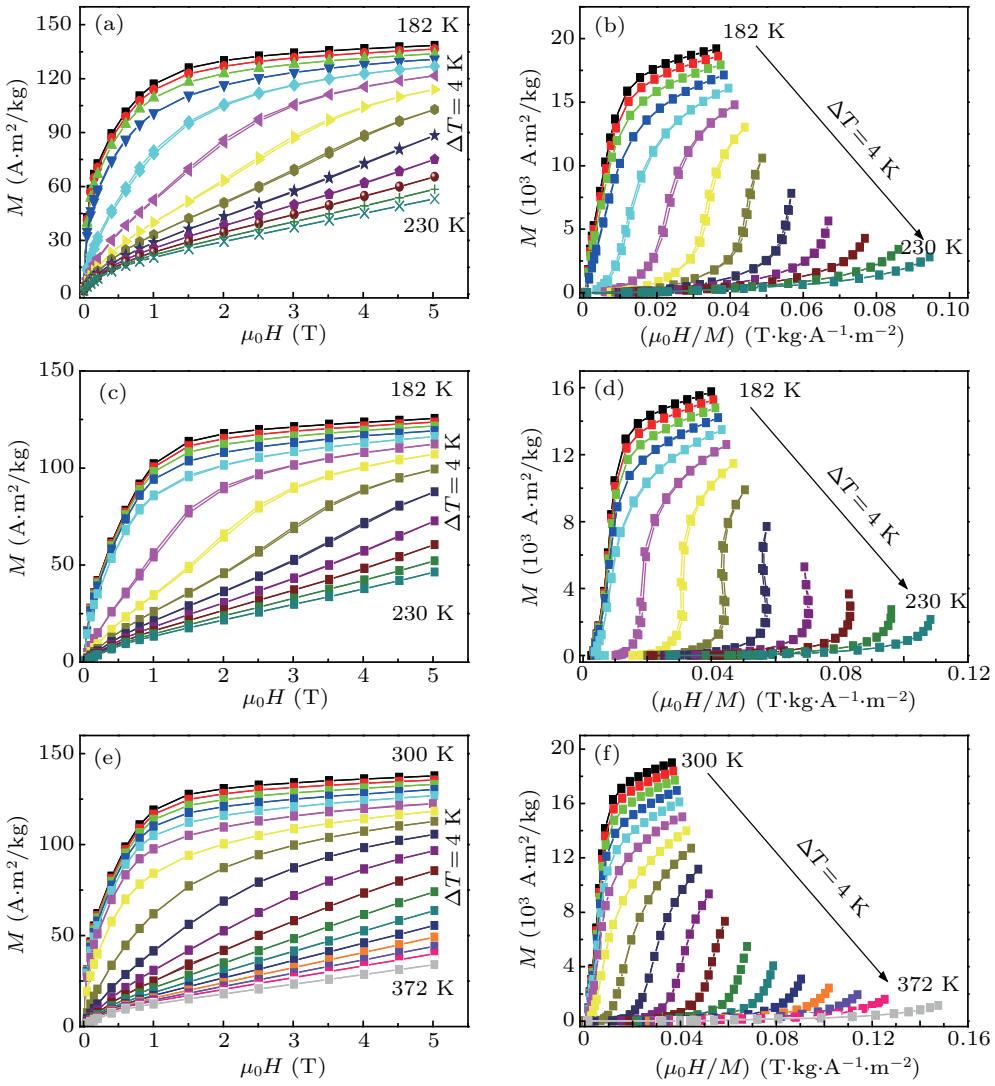


Fig. 5. (a), (c), (e) Isothermal magnetization curves measured with field increasing and decreasing around T_C and (b), (d), (f) Arrott plots of $La_{0.5}Pr_{0.5}Fe_{11.4}Si_{1.6}$ ribbons melt-spun at 30 m/s, then annealed and hydrogenated, respectively.

Figures 5(a), 5(c), and 5(e) show the isothermal magnetization curves measured in ascending and descending magnetic field around T_C of $La_{0.5}Pr_{0.5}Fe_{11.4}Si_{1.6}$ ribbons melt-spun at 30 m/s, then annealed and hydrogenated, respectively. It is shown that the magnetization of the ribbons decreases with temperature increasing. Figures 5(a)–5(c) exhibit that there is a small hysteresis in the isothermal magnetization curve. However, figure 5(e) shows that the magnetization curves of hydrogenated ribbons coincide completely in the field ascending process and the field descending process, revealing that

almost no hysteresis exists and the introduction of H atoms can weaken the field-induced phase transition. Figure 6 displays the hysteresis losses at 5 T as a function of temperature for these ribbons, and these hysteresis losses are obtained by calculating the enclosed area between magnetizing and demagnetizing curves. The values of maximum hysteresis losses reach 4.1 J/kg, 3.9 J/kg, and 0.6 J/kg for these ribbons. Here, the hysteresis loss lower than the hysteresis losses of bulk ingots is due to the homogenized chemical composition and microstructure for the ribbons melt-spun at 30 m/s.[13] Figures 5(b), 5(d), 5(f) display the Arrott plots of these ribbons melt-spun at 30 m/s, then annealed and hydrogenated, respectively. The negative slopes are found in Figs. 5(b) and 5(d), indicating the existence of the first-order field-induced IEM transition from PM to FM state.[28] For hydrogenated ribbons, weakened negative slopes demonstrate that the characteristic of the first-order magnetic transition is lessened after having been hydrogenated. Therefore, the introduction of H atoms into $La_{0.5}Pr_{0.5}Fe_{11.4}Si_{1.6}$ brings about a smaller hysteresis loss.

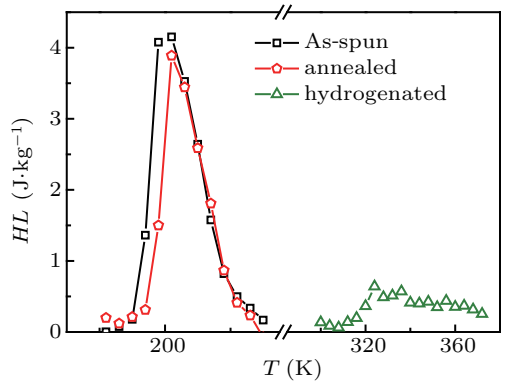


Fig. 6. Hysteretic loss (*HL*) under a magnetic field change of 0 T–5 T as a function of temperature for $La_{0.5}Pr_{0.5}Fe_{11.4}Si_{1.6}$ melt-spun ribbons, then respectively annealed and hydrogenated ribbons for wheel speed 30 m/s.

Gschneidner *et al.* proposed the relative cooling power (RCP) as an important parameter to evaluate MCE,[29] which usually reflects the refrigerant capacity of magnetocaloric material in a thermodynamic cycle. The relative cooling capacity is calculated from the following equation:

$$\mathrm{RCP} = -\Delta(S_{\mathrm{M}})_{\max} \cdot \Delta T_{\mathrm{FWHM}}, \tag{2}$$

where ΔT_{FWHM} is the full width at half-maximum of the ΔS–T curve. The values of refrigerant capacity for a field change of 0 T–5 T are 416.2 J/kg, 361.4 J/kg, and 412.5 J/kg for the ribbons listed in Table 1. Meanwhile, we calculate the average hysteretic losses (*A-HL*) of the three ribbons because the *A-HL* is another factor quantifying the potential of MCE of material. The values of *A-HL* are 2.9 J/kg, 2.6 J/kg, and 0.4 J/kg for these ribbons, as calculated by integrating the area under the curves of hysteresis loss in the same temperature range as RCP. The net RCP is calculated by subtracting *A-HL* from RCP. The values of RCP, *A-HL* and the net RCP for these ribbons are all listed in Table 1. The values of the net RCP for these ribbons are equal to or higher than those of materials with the first-order magnetic transition around room temperature for a field change of 0 T–5 T, such as $Gd_5Ge_{1.9}Si_2Fe_{0.1}$ (about 355 J/kg at 305 K),[30] $LaFe_{11.0}Co_{0.9}Si_{1.1}$ (about 275 J/kg at 294 K),[31] $Ni_{50}Mn_{34}In_{16}$ (about 181 J/kg at 304 K).[32] Our work demonstrates that the $La_{0.5}Pr_{0.5}Fe_{11.4}Si_{1.6}$ hydride ribbons with the large values of $-\Delta S_{\mathrm{M}}$ and RCP, small hysteresis loss can be used as magnetic refrigerant near room temperature.

Table 1. Values of Curie temperature (T_{C}), magnetic entropy change ($-\Delta S_{\mathrm{M}}$), relative cooling power (RCP), average hysteresis loss (*A-HL*) for $La_{0.5}Pr_{0.5}Fe_{11.4}Si_{1.6}$ ribbons for wheel speed 30 m/s, then annealed and hydrogenated, respectively.

30 m/s	$-\Delta S_{\mathrm{M}}$ (J/kg·K)	RCP (J/kg)	*A-HL* (J/kg)	net RCP (J/kg)
As-spun ribbons	18.1	416.2	2.9	413.3
Annealed ribbons	17.3	361.4	2.6	358.7
Hydrogenated ribbons	17.9	412.5	0.4	4121

4. Conclusions

The $La_{0.5}Pr_{0.5}Fe_{11.4}Si_{1.6}$ ribbons are prepared by using melt-spun with different wheel speeds and subsequent annealing, high-pressure hydrogenation treatment. The phase constituents, microstructure and magnetocaloric properties of the $La_{0.5}Pr_{0.5}Fe_{11.4}Si_{1.6}$ ribbons are studied under different processing conditions. It is found that the increase of wheel speed is beneficial to the formation of $NaZn_{13}$-type phase and refinement of grain size. The optimal wheel speed is determined to be 30 m/s based on the XRD and microstructural analysis. A largest entropy change of 18.1 J/kg·K at 190 K under a magnetic field change of 0 T–5 T is obtained in $La_{0.5}Pr_{0.5}Fe_{11.4}Si_{1.6}$ ribbons melt-spun at wheel speed 30 m/s. After a high-pressure (50 MPa) hydrogenation treatment, the Curie temperature of the ribbons melt-spun at 30 m/s is adjusted to about 314 K. The large $-\Delta S_{\mathrm{M}}$ of 17.9 J/kg·K and the net *RCP* of 412 J/kg with almost no hysteresis loss are maintained under the same magnetic field change around room temperature. The small thermal and magnetic hysteresis, the large value of magnetic entropy change and cooling power make the $La_{0.5}Pr_{0.5}Fe_{11.4}Si_{1.6}$ hydride ribbons a promising alternative to magnetic refrigeration around room temperature.

References

[1] Pecharsky V K and Gschneidner K A 1997 *Phys. Rev. Lett.* **78** 4494
[2] Tegus O, Bruck E, Buschow K H J and de Boer F R 2002 *Nature* **415** 150
[3] Bao L F, Hu F X, Chen L, Wang J, Sun J R and Shen B G 2012 *Appl. Phys. Lett.* **101** 162406
[4] He C, Zhang M X, Shao Y Y, Dong J D, Yan A R and Liu J 2015 *Chin. Phys. B* **24** 077503
[5] Chen Y F, Wang F, Shen B G, Hu F X, Cheng Z H, Wang G J and Sun J R 2002 *Chin. Phys.* **11** 741

[6] Shen B G, Sun J R, Hu F X, Zhang H W and Cheng Z H 2009 *Adv. Mater.* **21** 4545
[7] Xu L, Zhao J L, Yang J J, Zhang H G, Liu D M, Yue M and Jang Y J 2017 *Chin. Phys. B* **26** 067502
[8] Niitsu K and Kainuma R 2012 *Intermetallics* **20** 160
[9] Liu J, Krautz M, Skokov K, Woodcock T G and Gutfleisch O 2011 *Acta Mater.* **59** 3602
[10] Yang L, Li J, Tu D F, Strickland J C J, Hu Q D, Dong H B and Li J G 2020 *Acta Metall. Sin. (Engl. Lett.)* **33** 1535
[11] Zhang H, Hu F X, Sun J R and Shen B G 2013 *Sci. China: Phys. Mech. Astron.* **56** 2302
[12] Zhang P, Liu J, Shao Y and Yan A 2017 *Mater. Lett.* **193** 34
[13] Yan A, Muller K H and Gutfleisch O 2005 *J. Appl. Phys.* **97** 036102
[14] Yang J, Shao Y Y, Feng Z X and Liu J 2018 *J. Magn. Magn. Mater.* **452** 473
[15] Hou X L, Han N, Xue Y, Lu Q Q, Wang X C and Phan M H 2016 *J. Electron. Mater.* **45** 4730
[16] Santana R P, de Oliveira N A and von Ranke P J 2011 *J. Alloys Compd.* **509** 6346
[17] Yan A, Mueller K H and Gutfleisch O 2008 *J. Alloys Compd.* **450** 18
[18] Shen J, Li Y X, Wang F, Wang G J and Zhang S Y 2004 *Chin. Phys.* **13** 1134
[19] Fujita A, Fujieda S, Hasegawa Y and Fukamichi K 2003 *Phys. Rev. B* **67** 104416
[20] Sun N K, Guo J, Zhao X G, Si P Z, Huang J H and Zhang Z D 2015 *Appl. Phys. Lett.* **106** 092401
[21] Hou X L, Xue Y, Liu C Y, Xu H, Han N, Ma C W and Phan M H 2015 *Nanoscale Res. Lett.* **10** 1
[22] Liu X B, Altounian Z and Tu G H 2004 *J. Phys.: Condes. Matter* **16** 8043
[23] Fujieda S, Fukamichi K and Suzuki S 2013 *J. Alloys Compd.* **566** 196
[24] Shen J, Gao B, Zhang H W, Hu F X, Li Y X, Sun J R and Shen B G 2007 *Appl. Phys. Lett.* **91** 142504
[25] Zhao J L, Shen J, Hu F X, Li Y X, Sun J R and Shen B G 2010 *J. Appl. Phys.* **107** 113911
[26] Rosca M, Balli M, Fruchart D, Gignoux D, Hlil E K, Miraglia S, Ouladdiaf B and Wolfers P 2010 *J. Alloys Compd* **490** 50
[27] Moze O, Kockelmann W, Liu J P, de Boer F R and Buschow K H J 1999 *J. Magn. Magn. Mater.* **195** 391
[28] Hu F X, Shen B G, Sun J R, Cheng Z H, Rao G H and Zhang X X 2001 *Appl. Phys. Lett.* **78** 3675
[29] Gschneidner K A, Pecharsky V K and Tsokol A O 2005 *Rep. Prog. Phys.* **68** 1479
[30] Provenzano V, Shapiro A J and Shull R D 2004 *Nature* **429** 853
[31] Balli M, Fruchart D and Gignoux D 2007 *J. Phys.: Condes. Matter* **19** 236230
[32] Sharma V K, Chattopadhyay M K and Roy S B 2007 *J. Phys. D-Appl. Phys.* **40** 1869